Journal of The Physical Society of Japan
Vol. 60, No. 5, May, 1991, pp. 1814–1823

Piezooptical Studies of Group 4B Transition Metal Disulfides ZrS_2 and HfS_2*

Koichi TERASHIMA** and Isamu IMAI

Department of Pure and Applied Sciences, College of Arts and Sciences, University of Tokyo, Komaba, Meguro-ku, Tokyo 153

(Received December 13, 1990)

Piezotransmission spectra near the indirect absorption edge and piezoreflectance spectra in the visible region of group 4B transition metal disulfides ZrS_2 and HfS_2 have been studied by the stress modulation technique at 77 K. The uniaxial stress X was applied along the a axis and the spectra were measured using the polarized light, $E /\!/ X$ and $E \perp X$, where E is the electric field of the incident light. The change of the energy levels by the strain is evaluated by comparing the piezo-modulated spectra with the wavelength-modulated spectra. The main peak and the broad structure at higher energy side in the spectra originate from the overlapping of the transitions at and near Γ point and the other structures at lower energy side are due to the transitions at L and M points.

[piezotransmission, piezoreflectance, zirconium sulfide, hafnium sulfide, stress dichroism]

§1. Introduction

The layer type transition metal dichalcogenides are very attractive materials for their characteristic crystal structures and variety of physical properties.[1,2] Among them, group 4B transition metal disulfides ZrS_2 and HfS_2 are semiconductors with indirect band gap in the visible region. They crystallize in the CdI_2 type of layer structure. One layer consists of a plane of metal atoms sandwitched between two planes of sulfur atoms and the layers stack along the c axis. Within a layer each metal atom is octahedrally surrounded by six sulfur atoms. The bonding between atoms in the layers is covalent or ionic, while the bonding between the layers is of relatively weak van der Waals forces. So the crystal is easily cleaved along the layers. The crystal structure of ZrS_2 and HfS_2 belongs to space group D_{3d}^3.

After the pioneering work by Greenaway and Nitsche,[3] many experiments on the optical properties of the group 4B transition metal dichalcogenides including ZrS_2 and HfS_2 have been reported.[4–13] Absorption measurements indicate the indirect energy gap for ZrS_2 and HfS_2.[3–5] We have already reported the detailed natures of the absorption edges of ZrS_2 and HfS_2.[14] In that report, we have been led to the conclusion that the structures observed in the wavelength-modulated transmission spectra of ZrS_2 and HfS_2 are due to the indirect allowed transitions, $\Gamma_2^- \rightarrow L_1^+$ and $\Gamma_2^- \rightarrow M_1^+$, with excitonic effects.

Reflectance spectra of ZrS_2 and HfS_2 show several characteristic structures in the visible region.[7–10] These structures have been studied by a variety of experimental techniques and various assignments for these structures have been proposed. However, conclusive results concerning origins of these structures have not been obtained. For example, Bayliss and Liang[8] assigned the main peak at 3.30 eV in the reflectance of HfS_2 to the $\Gamma_3^- \rightarrow \Gamma_3^+$ transitions, while Fong *et al.*[7] assigned it to the transitions at R point in the Brillouin zone.

The calculations of the band structures of ZrS_2 and HfS_2 have been performed by many authors.[15–18] The valence band is made up

* Based on part of a thesis presented to the University of Tokyo in partial fulfillment of the degree of Doctor of Science by one of the authors (K. T.).

** Present address: Microelectronics Research Laboratories, NEC Corporation, 1-1, Miyazaki 4-chome, Miyamae-ku, Kawasaki, Kanagawa 213.

mainly of the p orbitals of the sulfur atoms and the conduction band is made up mainly of the d orbitals of the metal atoms. Their results indicate the existence of the indirect energy gap and also give the informations for the assignments of the structures in the reflectance spectra to the interband transitions.

In this paper, we report the results of the piezooptical measurements of ZrS_2 and HfS_2 in the visible region at 77 K. The effects of the strain and the possible assignments of the structures observed in the reflectance spectra are discussed.

§2. Experimental

Single crystals of ZrS_2 and HfS_2 were grown by the iodine vapour transport method. First of all, the powders of pure ZrS_2 and HfS_2 were made by the reaction of the pure elements in a sealed quartz ampoule at 900°C. Then the powder was put in another sealed quartz ampoule together with some amount of iodine. The ampoule was placed in the temperature gradient of a two zone furnace for single crystal growth. The temperatures of hot and cold part of the furnace were 950°C and 850°C for HfS_2 and 850°C and 750°C for ZrS_2, respectively. The growth time was about 150 h for both materials. The single crystals obtained were thin platelets with typical areas of 1 cm^2 and thickness of less than 200 μm.

In the piezooptical measurements, the cleaved sample was glued onto a fused quartz plate with the transparent silicone grease and this plate was attached along a diameter of the ring type piezoelectric transducer of lead-zirconate-titanate. The sample was mounted in a glass cryostat and immersed directly in liquid nitrogen. Alternating stress was applied to the sample along the a axis and the frequency was about 270 Hz. The voltage applied to the transducer was 700 V r.m.s..

The light from a tungsten lamp (50 W) was passed through a monochromator (SPEX 1704 with a 1200 grooves/mm grating) and polarized by a Rochon prism. The configurations of the electric field $\boldsymbol{E}$ of the incident light were ($\boldsymbol{E}\perp c$, $\boldsymbol{E}\perp \boldsymbol{X}$) and ($\boldsymbol{E}\perp c$, $\boldsymbol{E}/\!/\boldsymbol{X}$), where $\boldsymbol{X}$ is the applied stress. The light was focused on the surface of the sample at near normal incidence and was reflected or transmitted toward a photomultiplier. The dc component and the ac component of the reflected or transmitted light were measured directly and with a lock-in amplifier, respectively. The spectral width was kept less than 1 meV in the measurements of the reflectance and less than 3 meV in the transmission near the absorption edge.

The wavelength-modulated spectra were also measured in this work. The procedure of the measurements and the analysis of the data were almost the same as those already reported in the experiments of the transmission and its modulated spectra.[14]

§3. Theory

In this section, the effects of the stress on the optical properties of the samples are considered based on the theory of elastic body.[19,20] The thin sample was glued onto a rather thick fused quartz plate and this quartz plate was attached firmly to the piezoelectric transducer. The strain e^Q of the quartz plate is expressed using the compliance tensor s^Q of the quartz and the applied stress X as follows:

$$\begin{pmatrix} e^Q_{xx} \\ e^Q_{yy} \\ e^Q_{zz} \\ 2e^Q_{yz} \\ 2e^Q_{zx} \\ 2e^Q_{xy} \end{pmatrix} = \begin{pmatrix} s^Q_{11} & s^Q_{12} & s^Q_{12} & 0 & 0 & 0 \\ s^Q_{12} & s^Q_{11} & s^Q_{12} & 0 & 0 & 0 \\ s^Q_{12} & s^Q_{12} & s^Q_{11} & 0 & 0 & 0 \\ 0 & 0 & 0 & s^Q_{44} & 0 & 0 \\ 0 & 0 & 0 & 0 & s^Q_{44} & 0 \\ 0 & 0 & 0 & \mathrm{p} & 0 & s^Q_{44} \end{pmatrix} \begin{pmatrix} X \\ 0 \\ 0 \\ 0 \\ 0 \\ 0 \end{pmatrix} = \begin{pmatrix} s^Q_{11} \\ s^Q_{12} \\ s^Q_{12} \\ 0 \\ 0 \\ 0 \end{pmatrix} X, \tag{1}$$

where we take the x axis parallel to the stress X and the z axis perpendicular to the quartz plate. The a axis of the sample glued onto the quartz plate was along the x axis and the c axis along the z axis. As the thickness of the sample is very small, it can be assumed that the stress and the strain

in the sample are uniform and that the strain components e_{ij} of the sample in the xy plane are the same as e_{ij}^{Q} given by eq. (1), $e_{xx}=e_{xx}^{Q}$, $e_{yy}=e_{yy}^{Q}$, $e_{xy}=e_{xy}^{Q}$. The stress components X_{zz}, X_{yz}, and X_{zx} in the sample can be assumed to be very small or zero, because the opposite surface of the sample was kept free. Then the strain $\boldsymbol{e}$ in the sample is expressed using the compliance tensor $\boldsymbol{s}$ of the sample (the crystal structure of ZrS_2 and HfS_2 belongs to space group D_{3d}^{3}) as follows:

$$\begin{pmatrix} e_{xx} \\ e_{yy} \\ e_{zz} \\ 2e_{yz} \\ 2e_{zx} \\ 2e_{xy} \end{pmatrix} = \begin{pmatrix} s_{11} & s_{12} & s_{13} & s_{14} & 0 & 0 \\ s_{12} & s_{11} & s_{13} & -s_{14} & 0 & 0 \\ s_{13} & s_{13} & s_{33} & 0 & 0 & 0 \\ s_{14} & -s_{14} & 0 & s_{44} & 0 & 0 \\ 0 & 0 & 0 & 0 & s_{44} & 2s_{14} \\ 0 & 0 & 0 & 0 & 2s_{14} & 2(s_{11}-s_{12}) \end{pmatrix} \begin{pmatrix} X_{xx} \\ X_{yy} \\ 0 \\ 0 \\ 0 \\ X_{xy} \end{pmatrix}. \tag{2}$$

As mentioned above, e_{xx}, e_{yy}, and e_{xy} of the sample are equal to the corresponding strain components of the quartz plate. Since $2e_{xy}=2(s_{11}-s_{12})X_{xy}=2e_{xy}^{Q}=0$ is derived from eqs. (1) and (2), X_{xy} in the sample is zero. Then we can obtain the following expression for the strain of the sample:

$$\begin{pmatrix} e_{xx} \\ e_{yy} \\ e_{zz} \\ 2e_{yz} \\ 2e_{zx} \\ 2e_{xy} \end{pmatrix} = \begin{pmatrix} s_{11}^{Q} \\ s_{12}^{Q} \\ (s_{11}^{Q}+s_{12}^{Q})s_{13}/(s_{11}+s_{12}) \\ (s_{11}^{Q}-s_{12}^{Q})s_{14}/(s_{11}-s_{12}) \\ 0 \\ 0 \end{pmatrix} X. \tag{3}$$

Equation (3) can be rewritten as

$$\begin{pmatrix} e_{xx} \\ e_{yy} \\ e_{zz} \\ 2e_{yz} \\ 2e_{zx} \\ 2e_{xy} \end{pmatrix} = \frac{1}{2}(s_{11}^{Q}+s_{12}^{Q})X \begin{pmatrix} 1 \\ 1 \\ 0 \\ 0 \\ 0 \\ 0 \end{pmatrix} + \frac{(s_{11}^{Q}+s_{12}^{Q})s_{13}}{s_{11}+s_{12}} X \begin{pmatrix} 0 \\ 0 \\ 1 \\ 0 \\ 0 \\ 0 \end{pmatrix}$$

$$+\frac{1}{2}(s_{11}^{Q}-s_{12}^{Q})X \begin{pmatrix} 1 \\ -1 \\ 0 \\ 0 \\ 0 \\ 0 \end{pmatrix} + \frac{(s_{11}^{Q}-s_{12}^{Q})s_{14}}{s_{11}-s_{12}} X \begin{pmatrix} 0 \\ 0 \\ 0 \\ 1 \\ 0 \\ 0 \end{pmatrix}. \tag{4}$$

Equation (4) shows the expression of the strain of the sample decomposed into the irreducible components. The first and the second terms of the right-hand side of eq. (4) are the strains which give rise to a volume change without destroying the crystal symmetry and the third and the fourth terms are the strains which lower the crystal symmetry.

The optical properties of the crystal are described by the dielectric constant and the dependence of the dielectric tensor ε on the strain can be expressed as

$$\varepsilon(e)=\varepsilon(0)+\Delta\varepsilon(e). \tag{5}$$

The $\Delta\varepsilon(e)$ is related to the strain by the elastooptical tensor W.[19,20] For ZrS_2 and HfS_2, the relation is

$$\begin{pmatrix} \Delta\varepsilon_{xx} \\ \Delta\varepsilon_{yy} \\ \Delta\varepsilon_{zz} \\ \Delta\varepsilon_{yz} \\ \Delta\varepsilon_{zx} \\ \Delta\varepsilon_{xy} \end{pmatrix} = \begin{pmatrix} W_{11} & W_{12} & W_{13} & W_{14} & 0 & 0 \\ W_{12} & W_{11} & W_{13} & -W_{14} & 0 & 0 \\ W_{31} & W_{31} & W_{33} & 0 & 0 & 0 \\ W_{41} & -W_{41} & 0 & W_{44} & 0 & 0 \\ 0 & 0 & 0 & 0 & W_{44} & W_{41} \\ 0 & 0 & 0 & 0 & W_{14} & (W_{11}-W_{12})/2 \end{pmatrix} \begin{pmatrix} e_{xx} \\ e_{yy} \\ e_{zz} \\ 2e_{yz} \\ 2e_{zx} \\ 2e_{xy} \end{pmatrix}. \tag{6}$$

From eqs. (4) and (6), we obtain and the following expressions:

$$\Delta\varepsilon_{xx}+\Delta\varepsilon_{yy}=(s^Q_{11}+s^Q_{12})(W_{11}+W_{12})X+\frac{2(s^Q_{11}+s^Q_{12})s_{13}}{s_{11}+s_{12}}W_{13}X, \tag{7}$$

$$\Delta\varepsilon_{xx}-\Delta\varepsilon_{yy}=(s^Q_{11}-s^Q_{12})(W_{11}-W_{12})X+\frac{2(s^Q_{11}-s^Q_{12})s_{14}}{s_{11}-s_{12}}W_{14}X. \tag{8}$$

Equation (7) implies that $\Delta\varepsilon_{xx}+\Delta\varepsilon_{yy}$ depends only on the strains of the first and the second terms of eq. (4), which do not change the crystal symmetry. On the other hand, eq. (8) shows $\Delta\varepsilon_{xx}-\Delta\varepsilon_{yy}$ depends only on the strains of the third and the fourth terms of eq. (4), which lower the crystal symmetry.

The change of the reflectance or the transmittance for the polarized light of $E/\!/X$ is described by $\Delta\varepsilon_{xx}$ and that for $E\perp X$ by $\Delta\varepsilon_{yy}$. So it is possible to distinguish the effects of the two different components of the strain by the measurements of the reflectance using the polarized light. From now on, we call the strain components which contribute to $\Delta\varepsilon_{xx}+\Delta\varepsilon_{yy}$ 'radial strain e_r' and those which contribute to $\Delta\varepsilon_{xx}-\Delta\varepsilon_{yy}$ 'uniaxial strain e_u'. The radial strain does not change the crystal symmetry and the main effect of them is the shifts of the energy levels in the band structure. The uniaxial strain lowers the crystal symmetry and may give rise the splittings as well as the shifts of the energy levels.

§4. Results and Discussion

Figures 1 and 2 show the spectra of the reflectance (R), the wavelength-modulated reflectance (WMR), and the piezoreflectance (PR) at 77 K for ZrS_2 and HfS_2, respectively. The structures in the reflectance spectra are indicated by the arrows. Corresponding to these structures, the WMR and the PR spectra show the characteristic features. In the WMR spectra, $\Delta R/R$ denotes the derivative of R with respect to the photon energy, that is $(1/R)\{dR/d(h\nu)\}$, where $h\nu$ is the photon energy. The PR spectra are shown for $E/\!/X$ and $E\perp X$, where E is the electric field of the incident light and X is the applied stress. In the PR spectra, the sign of $\Delta R/R$ is defined to be negative when R is increased by the tensile stress along the a axis. According to this definition, the structure in the R spectra shifts to higher energies by the tensile stress if the sign of PR signal is the same as that of WMR signal.

In the spectra of the reflectance for ZrS_2 and HfS_2, a main peak and some small peaks can be seen. The energies of the structures in the R spectra are listed in Table I. In the PR spectra, a large structure corresponding to the main peak in the R spectra and some small structures can be seen.

The PR spectra seem to be similar to the WMR spectra except that the sign and the relative intensity of each structure are different. In order to analyze the PR spectra and discuss the effect of the stress according to the results in §3, we take the sum and the difference of the spectra for the different polarizations of the light, that is, the sum and the difference of $(\Delta R/R)_{/\!/}$ for $E/\!/X$ and $(\Delta R/R)_\perp$ for $E\perp X$.

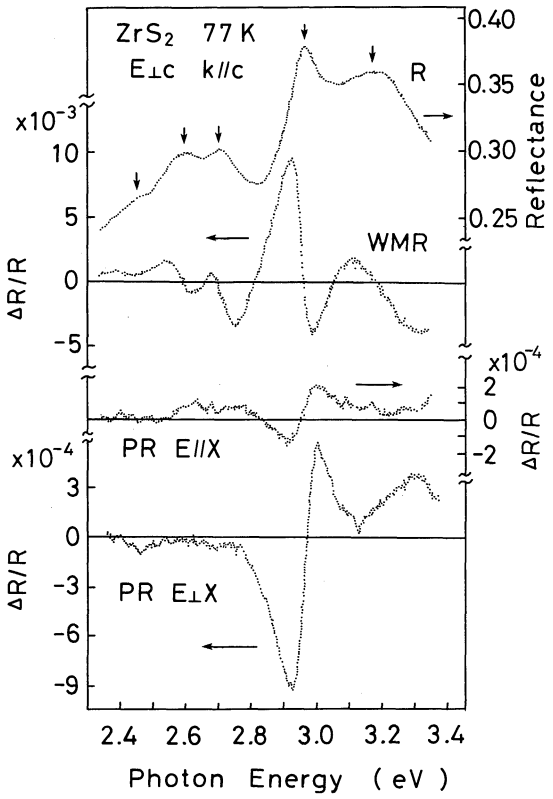

Fig. 1. The reflectance (R), the wavelength-modulated reflectance (WMR), and the piezoreflectance (PR) spectra at 77 K for ZrS_2. The structures in the reflectance are indicated by the arrows. In the WMR spectrum, $\Delta R/R$ denotes the derivative of R with respect to the photon energy. The PR spectra are shown for $E/\!/X$ and $E\perp X$, where E is the electric field of the incident light and X is the applied stress. In the PR spectra, the sign of $\Delta R/R$ is defined to be negative when R is increased by the tensile stress along the a axis.

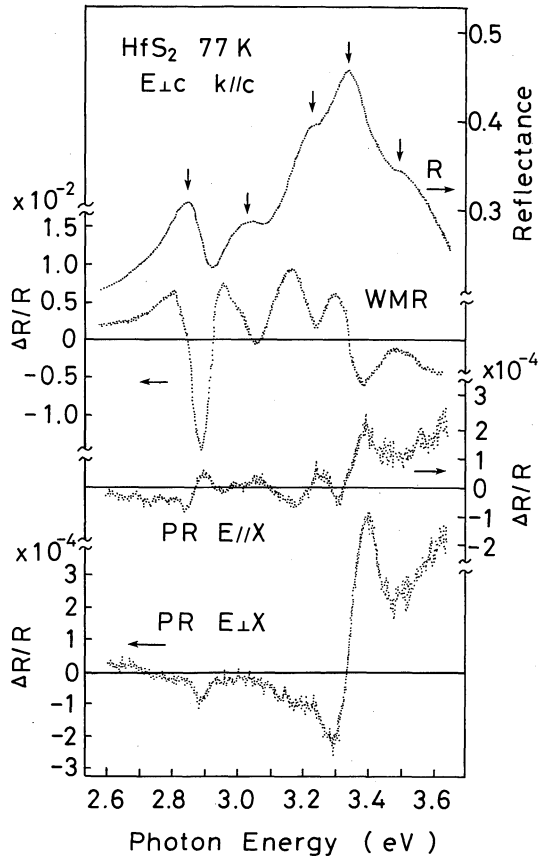

Fig. 2. The reflectance (R), the wavelength-modulated reflectance (WMR), and the piezoreflectance (PR) spectra at 77 K for HfS_2.

Table I. The structures in the reflectance spectra of ZrS_2 and HfS_2.

	ZrS_2		HfS_2	
1.	2.44 eV	small shoulder	2.85 eV	sharp peak
2.	2.60 eV	small peak	3.02 eV	shoulder
3.	2.71 eV	small peak	3.22 eV	shoulder
4.	2.97 eV	main peak	3.34 eV	main peak
5.	3.17 eV	broad peak	3.49 eV	broad shoulder

The results are shown in Figs. 3 and 4. In these figures, $(\Delta R/R)_{/\!/}+(\Delta R/R)_{\perp}$ reflects the effects of the radial strain which keeps the crystal symmetry unchanged, and $(\Delta R/R)_{/\!/}-(\Delta R/R)_{\perp}$ represents the effects of the uniaxial strain which reduces the crystal symmetry as mentioned in §3. As can be seen in the spectra of $(\Delta R/R)_{/\!/}-(\Delta R/R)_{\perp}$, the stress dichroism appears for all the structures in the reflectance spectra.

Also for the transmission spectra in the lower photon energy region, the same procedure of the analysis is taken as the case of the reflectance. Figures 5 and 6 show the wavelength-modulated transmission (WMT) spectra and the sum and the difference of the piezotransmission (PT) spectra for the different polarization of the light, $(\Delta T/T)_{/\!/}+(\Delta T/T)_{\perp}$ and $(\Delta T/T)_{/\!/}-(\Delta T/T)_{\perp}$. In Fig. 5 for ZrS_2, the small structure near 1.9 eV in the WMT spectra cannot be seen in the PT spectra. The reason may be the higher noise level and the lower spectral resolution in the

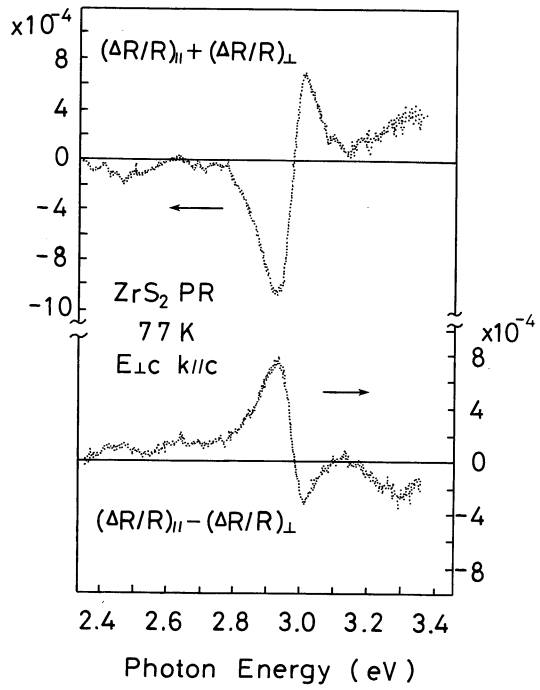

Fig. 3. The sum and the difference of the *PR* spectra of ZrS_2 for the different polarizations of the light. $(\Delta R/R)_{//}$ is the *PR* spectra for $E//X$ and $(\Delta R/R)_{\perp}$ is for $E\perp X$.

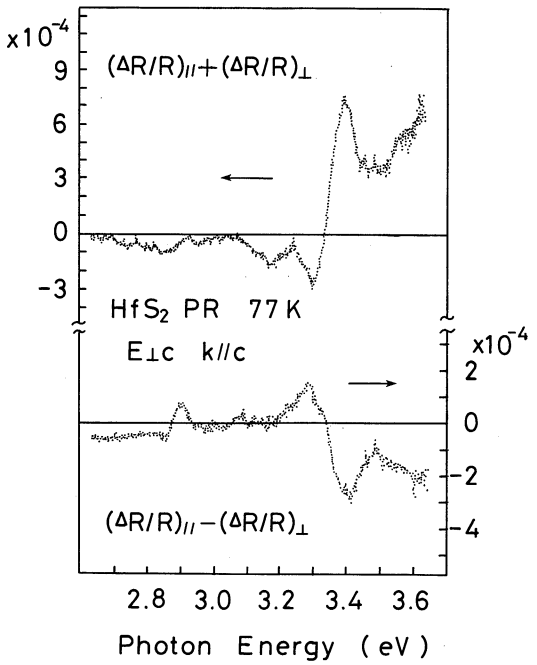

Fig. 4. The sum and the difference of the *PR* spectra of HfS_2 for the different polarizations of the light.

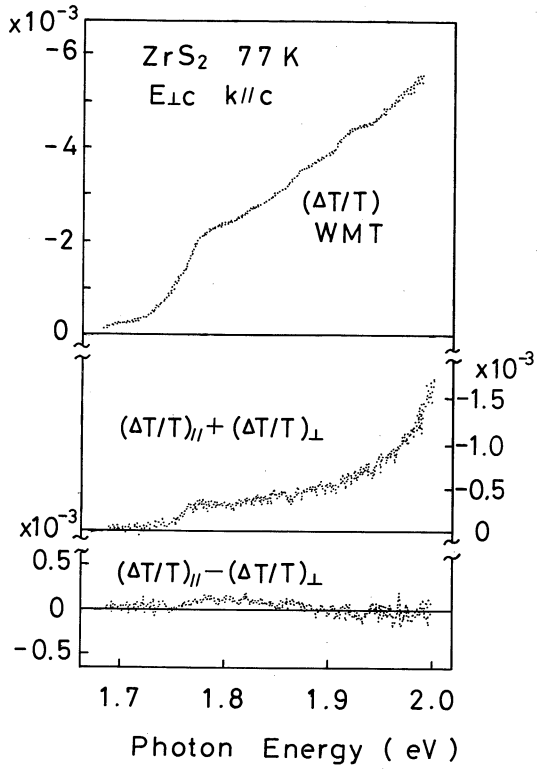

Fig. 5. The wavelength-modulated transmission (*WMT*) and the piezotransmission (*PT*) spectra at 77 K for ZrS_2. The sum and the difference of the *PT* spectra for the different polarization are shown.

PT measurements. As for the transmission, the stress dichroism is not so clear as the reflectance but some indications can be seen in the $(\Delta T/T)_{//} - (\Delta T/T)_{\perp}$ spectra.

In order to analyze the spectra quantitatively, we define strain coupling coefficients D_r and D_u as follows for the *PR* spectra:

$$D_r = \frac{(\Delta R/R)_{//} + (\Delta R/R)_{\perp}}{(\Delta R/R)_{WMR}} \times \frac{(\Delta E)_{WMR}}{2e_r}, \quad (9)$$

$$D_u = \frac{(\Delta R/R)_{//} - (\Delta R/R)_{\perp}}{(\Delta R/R)_{WMR}} \times \frac{(\Delta E)_{WMR}}{2e_u}, \quad (10)$$

where $(\Delta E)_{WMR}$ is the full width of the modulation of the photon energy in the *WMR* measurement and e_r and e_u are the amplitudes of the alternating strains applied in the *PR* measurement. The quantity $D_r e_r$ is the amplitude of the energy shift induced by the radial strain e_r and the quantity $D_u e_u$ is the energy splitting induced by the uniaxial strain e_u. Similarly, we define D_r and D_u for the *PT*

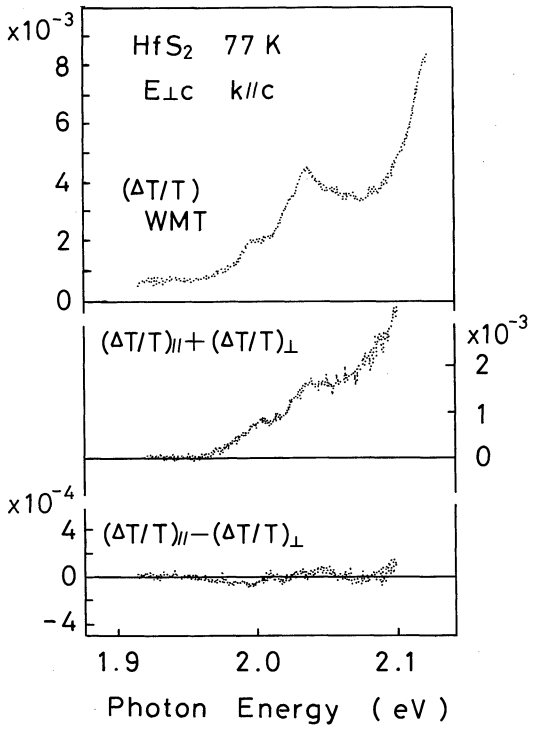

Fig. 6. The wavelength-modulated transmission (*WMT*) and the piezotransmission (*PT*) spectra at 77 K for HfS_2.

spectra as

$$D_r=\frac{(\Delta T/T)_{//}+(\Delta T/T)_{\perp}}{(\Delta T/T)_{WMR}}\times\frac{(\Delta E)_{WMT}}{2e_r}, \quad (11)$$

$$D_u=\frac{(\Delta T/T)_{//}-(\Delta T/T)_{\perp}}{(\Delta T/T)_{WMR}}\times\frac{(\Delta E)_{WMT}}{2e_u}, \quad (12)$$

where $(\Delta E)_{WMT}$ is the full width of the modulation of the photon energy in the *WMT* measurement.

The $(\Delta R/R)_{//}+(\Delta R/R)_{\perp}$ and the $(\Delta T/T)_{//}+(\Delta T/T)_{\perp}$ are the magnitudes of the observed signals generating by the radial strain e_r. As shown in §3, the radial strain e_r has two components, (1, 1, 0, 0, 0, 0) and (0, 0, 1, 0, 0, 0). The first one represents the uniform expansion in the plane perpendicular to the *c* axis. Its magnitude is determined entirely by the strain of the quartz plate to which the sample is attached and is independent on the elastic property of the sample. On the other hand, the second one is the strain along the *c* axis and its magnitude depends on the compliance tensor of the sample. The values of the compliance tensors of ZrS_2 and HfS_2 are not known. Thus, though the magnitude of the strain component (0, 0, 1, 0, 0, 0) cannot be determined, that of the strain component (1, 1, 0, 0, 0, 0) can be estimated from the known values of the compliance tensors of the quartz and the piezoelectric transducer, and from the applied voltage. In the similar way, the magnitude of the strain component (1, −1, 0, 0, 0, 0) can also be estimated. If we take only the strain components (1, 1, 0, 0, 0, 0) and (1, −1, 0, 0, 0, 0), we will find $e_r=3.4\times10^{-5}$ and $e_u=4.8\times10^{-5}$ in this experiment. These values would not vary so widely even if the strain components (0, 0, 1, 0, 0, 0) and (0, 0, 0, 1, 0, 0) are taken into account. Thus the values of D_r and D_u can be obtained using eqs. (9)-(12) and are listed in Table II.

We will discuss the assignments of the structures in the reflectance spectra by considering the values of D_r and D_u. First, it is noted that all the observed values of D_r are negative. This indicates that all the energy differences between the levels associated with the optical transitions are decreased by the radial strain.

Table II. Strain coupling coefficients for the structures in the transmittance and the reflectance spectra.

(a) ZrS_2

Position of the structure (eV)	D_r (eV/strain)	D_u (eV/strain)
Transmittance		
(1) 1.76	−1.8	−0.12
Reflectance		
(1) 2.44	−1.6	−0.86
(2) 2.60	−2.1	−1.7
(3) 2.71	−0.96	−0.35
(4) 2.97	−5.5	2.6
(5) 3.17	−3.3	1.3

(b) HfS_2

Position of the structure (eV)	D_r (eV/strain)	D_u (eV/strain)
Transmittance		
(1) 2.00	−3.3	−0.13
(2) 2.03	−3.0	−0.19
Reflectance		
(1) 2.85	−0.16	−0.12
(2) 3.02	−0.23	−0.10
(3) 3.22	−0.81	−0.14
(4) 3.34	−3.6	1.2
(5) 3.49	−3.6	0.88

In other words, the band gap is narrowed by the radial strain.

The values of D_r for the main peak and the broad structure at higher energy side are considerably larger than those for the other structures, especially in the case of HfS_2. In the transmission spectra, the values of D_r are also large for two structures for HfS_2, but not so large for ZrS_2. Moreover, the values of D_u for the main peak and the broad structure at higher energies are positive in contrast to the negative values for the other structures. This suggests that the characters of these two structures are different from those of the other structures.

Benesh *et al.*[21] calculated the band structures of TiS_2 and $TiSe_2$, which belong to the same group 4B transition metal dichalcogenides as ZrS_2 and HfS_2, under the hydrostatic pressure. According to their results, the top of the valence band at Γ point (Γ_2^- state) shifts to higher energies and the magnitude of the shift is larger than any other points in the Brillouin zone. They explained the reason of this behavior as follows: the Γ_2^- state is made up of the p_z orbitals of the chalcogen and spread over the layers through the van der Waals gap along the c axis. The deformation of the lattice along the c axis is larger than that along the a axis under the hydrostatic pressure. So the Γ_2^- state shifts more sensitively by the pressure.

The same behavior in ZrS_2 and HfS_2 may be expected under the pressure. However, it is noted that the stress applied in this experiment is different from the hydrostatic pressure. The ratio of the magnitudes of the strains along the c axis and along the a axis in the case of this work is expressed as

$$(\Delta c/c)/(\Delta a/a)=s_{13}/2(s_{11}+s_{12}). \qquad (13)$$

Unfortunately, the values of the compliance tensors of ZrS_2 and HfS_2 are not known. However, the ratio in eq. (13) can be known for the other materials with layered structures. For example, $(\Delta c/c)/(\Delta a/a)$ is -0.28 for PbI_2 and -0.20 for CdI_2. This indicates that the deformation of the lattice along the c axis is not so small under the uniaxial stress. When the lattice is deformed by the tensile stress along the a axis, the sign of $\Delta c/c$ is negative. This deformation of the lattice along the c axis is the same as the case of the hydrostatic pressure. Then the same behavior as in the case of the hydrostatic pressure, that is, the shift of the Γ_2^- state to higher energies, is expected under the tensile stress along the a axis.

Most of the band calculations[15-18] and the optical experiments[7-10] reported in the past reveal that the structures in the reflectance spectra in the visible region originate from mainly the transitions at Γ, L, and M points. Considering these facts and the above discussion, we are led to the conclusion that the structures whose value of D_r is large may be due to the transitions at Γ point and that the other structures may be related to L or M point. The relatively large values of D_r for the transmission may be explained as that Γ_2^- state is the initial state of the transitions in the absorption edge. The possible assignments of the main peak and the broad structure at higher energies are $\Gamma_2^- \rightarrow \Gamma_3^+$ and $\Gamma_3^- \rightarrow \Gamma_3^+$.

The other structures are assigned to the transitions at L and M points, $L_2^- \rightarrow L_1^+$, $L_1^- \rightarrow L_1^+$, and $M_1^- \rightarrow M_1^+$. The band calculations show that the order of the energies of these transitions are different between ZrS_2 and HfS_2. The transition with the lowest energy is $M_1^- \rightarrow M_1^+$ for ZrS_2 and $L_2^- \rightarrow L_1^+$ for HfS_2. The assignments have been made considering these facts.

However, taking the spin-orbit splitting into consideration, this conclusion cannot explain the effects of the uniaxial strain, D_u. All the structures in the spectra show the stress dichroism, that is, D_u is not zero. This indicates the energy levels associated with the optical transitions are split under the uniaxial strain. On the other hand, the Γ_3^- and the Γ_3^+ states are transformed into $\Gamma_{4,5}^{\mp}$ and $\Gamma_6^{\mp}$ by the spin-orbit interaction. As the $\Gamma_{4,5}^{\mp}$ and $\Gamma_6^{\mp}$ states are nondegenerate aside from spin, these energy levels at Γ point may not be split by the strain.

According to the relativistic band calculations,[15,18] the energy separations due to the spin-orbit interaction are 70 meV for the Γ_3^- of HfS_2, 150 meV for the Γ_3^+ of HfS_2, and 30 meV for the Γ_3^- of ZrS_2. These values, however, have not yet been confirmed by the experiments.

The splittings of the energy levels in the solid under the strain is possible. For example, the M point in the Brillouin zone of ZrS_2 and HfS_2 consists of the six equivalent points with the C_{2h} symmetry. When the crystal is strained by the stress applied along the a axis, the crystal symmetry is reduced and the six equivalent M points are split into two equivalent points with the C_{2h} symmetry and four equivalent points with the C_i symmetry. So the energy level at M point is split into two energy levels by the uniaxial strain. Such splittings may occur at several high symmetry points in the Brillouin zone.

Such a splitting does not occur at Γ point but it may occur at the points near Γ point, for example, Σ line. Therefore, the main peak and the broad structure at higher energies in the reflectance spectra may be considered to be the superposition of the optical transitions not only at Γ point but also at the points near Γ point (Δ, Σ, R, A). Rather broad peaks may be due to the overlapping of the transitions at these points and the spin-orbit splitting of the levels.

Also for the structures caused by the transitions at L and M points, the overlapping of the transitions near these points must be considered. However, the band structures of ZrS_2 and HfS_2 reveal that the energy dispersion is considerably strong near L and M points. Then such a overlapping may not be so significant.

Considering the above discussion and referring to the band calculations, we try to assign the structures in the reflectance spectra of ZrS_2 and HfS_2. In the course of the assignment, it was considered that the relatively large values of D_r is due to the large shift of the energy levels at Γ point under the strain. The stress dichroism can be explained by the stress induced splitting of the energy levels at the high symmetry points in the Brillouin zone. The results of the assignment are shown in Table III.

Table III. The assignments of the structures in the reflectance spectra of ZrS_2 and HfS_2.

(a) ZrS_2

	Position of the structure (eV)	Assignments
1.	2.44	$M_1^- \to M_1^+$
2.	2.60	$L_2^- \to L_1^+$
3.	2.71	$L_1^- \to L_1^+$
4.	2.97	$\Gamma_2^- \to \Gamma_3^+$ and the transitions near Γ
5.	3.17	$\Gamma_3^- \to \Gamma_3^+$ and the transitions near Γ

(b) HfS_2

	Position of the structure (eV)	Assignments
1.	2.85	$L_2^- \to L_1^+$
2.	3.02	$L_1^- \to L_1^+$
3.	3.22	$M_1^- \to M_1^+$
4.	3.34	$\Gamma_2^- \to \Gamma_3^+$ and the transitions near Γ
5.	3.49	$\Gamma_3^- \to \Gamma_3^+$ and the transitions near Γ

§5. Summary and Conclusions

The piezotransmission and the piezoreflectance spectra of ZrS_2 and HfS_2 have been measured. The uniaxial stress X is applied along the a axis. The sum of the spectra for the different directions of the polarization $(\Delta T/T)_{/\!/}+(\Delta T/T)_{\perp}$ and $(\Delta R/R)_{/\!/}+(\Delta R/R)_{\perp}$, shows the effect of the radial strain and the difference, $(\Delta T/T)_{/\!/}-(\Delta T/T)_{\perp}$ and $(\Delta R/R)_{/\!/}-(\Delta R/R)_{\perp}$, shows the effect of the uniaxial strain. The effect of the radial strain is expressed quantitatively as the shift of the energy level and that of the uniaxial strain is expressed as the splitting of the energy level.

The main peak and the broad structure at higher energy side in the reflectance spectra show the large D_r with negative sign and the relatively large D_u with positive sign. These structures are assigned to the transitions at and near Γ point. The other structures at lower energy side are assigned to the transitions at L and M points.

References

1) J. A. Wilson and A. D. Yoffe: Adv. Phys. **18** (1969) 193.
2) A. D. Yoffe: Festkorperprobleme **13** (1973) 1.
3) D. L. Greenaway and R. Nitsche: J. Phys. Chem. Solids **26** (1965) 1445.
4) P. A. Lee, G. Said, R. Davis and T. H. Lim: J. Phys. Chem. Solids **30** (1969) 2719.
5) J. Camassel, S. Kohn, Y. R. Shen and F. Levy: Nuovo Cimento **38B** (1977) 185.
6) A. R. Beal, J. C. Knights and W. Y. Liang: J. Phys. C (Solid State Phys.) **5** (1972) 3531.

7) C. Y. Fong, J. Camassel, S. Kohn and Y. R. Shen: Phys. Rev. B**13** (1976) 5442.
8) S. C. Bayliss and W. Y. Liang: J. Phys. C (Solid State Phys.) **15** (1982) 1283.
9) A. Burghesi, Chen Chen-jia, G. Guizzetti, L. Nosenzo, E. R. Reguzzoni, A. Stella and F. Levy: Phys. Rev. B**33** (1986) 2422.
10) G. Peloquin, R. Provencher, S. Jandl and M. Aubin: J. Phys. C (Solid State Phys.) **19** (1986) 3141.
11) R. Mamy, B. Thieblemont and O. Cerclier: J. de Phys. Lett. **37** (1976) L85.
12) R. Mamy, B. Thieblemont, L. Martin and F. Pradal: Nuovo Cimento **38**B (1977) 196.
13) H. P. Hughes and W. Y. Liang: J. Phys. C (Solid State Phys.) **10** (1977) 1079.
14) K. Terashima and I. Imai: J. Phys. Soc. Jpn. **59** (1990) 738.
15) R. B. Murray, R. A. Bromley and A. D. Yoffe: J. Phys. C (Solid State Phys.) **5** (1972) 746.
16) L. F. Mattheiss: Phys. Rev. B**8** (1973) 3719.
17) H. M. Isomaki and J. von Boehm: Phys. Lett. **89**A (1982) 89.
18) J. von Boehm and H. M. Isomaki: J. Phys. C (Solid State Phys.) **15** (1982) L733.
19) J. F. Nye: *Physical Properties of Crystals* (Oxford Univ. Press, London and New York, 1957).
20) I. Balslev: *Semiconductors and Semimetals* (Academic Press, New York and London, 1972) Vol. 9, p. 403.
21) G. A. Benesh, A. M. Woolley and C. Umrigar: J. Phys. C (Solid State Phys.) **18** (1985) 1595.